

Silver Clusters Embedded in Glass as a Perennial High Capacity Optical Recording Medium

By Arnaud Royon, Kevin Bourhis, Matthieu Bellec, Gautier Papon, Bruno Bousquet, Yannick Deshayes, Thierry Cardinal, and Lionel Canioni*

Preceding civilizations succeeded in transmitting their cultural heritage, using first stone and then paper as storage media. Paradoxically, our numerical civilization, which produces a lot more information and knowledge, has not answered this challenge yet. Current magnetic and optical recording media have improved in terms of storage capacity and access speed over the past decades. Nevertheless, they suffer from a critical drawback: their lifetime. A recent study has revealed that these media have a lifetime no longer than five to ten years.^[1] On the one hand, magnetic media mainly suffer from high sensitivity to electromagnetic radiation and can accidentally “crash”. On the other hand, current optical media have limited storage capacity and material durability.

The demand for increasing optical information storage capacity follows the progress achieved in data transfer and handling. CDs, DVDs and “Blu-ray” discs are two-dimensional (2D) data storage media, which can support only a few layers. Among all the current commercially available optical data storage supports, the “Blu-ray” disc is the one which presents the highest capacity, up to 50 Gbytes. The “super resolution” technique could even increase this capacity to a theoretical limit of 100 Gbytes.^[2] Another 2D optical recording medium has been proposed, the holographic versatile disk (HVD), with a higher storage capacity (up to 10 Tbytes).^[3] Nevertheless, it has a prohibitive cost and no commercially available drive yet. To overcome the storage capacity limitation, the next generation of optical recording media should be 3D or more, in order to increase significantly the data density. Dimensions such as space,^[4,5] phase,^[4] wavelength,^[5,6] polarization,^[5,7] and fluorescence^[8] have been considered. Each of these techniques could increase the density beyond terabits per cubic centimeters (Tbit cm⁻³), but they suffer from commercially unavailable and expensive drive technologies.

Different 3D writing and reading techniques have been proposed, including multiphoton^[4] or confocal^[8] configurations. Femtosecond lasers are now a mature technology emerging on the market. They can deliver high peak powers while keeping low average powers. This particularity makes them perfectly suitable for local interaction and 3D patterning. 3D optical recording techniques rely either on photochromism or on fluorescence. Photochromism is defined as a reversible transformation of a single chemical species between two states that lead to different absorption and refractive index. This enables light characteristics such as wavelength, polarization, and phase to be multiplexed.^[9] 3D photochromism recording in photopolymers,^[4] photobleaching polymers,^[8,10] and void creation in transparent materials^[11,12] has been demonstrated using a femtosecond laser. On the other hand, fluorescence recording has been shown in dye-doped polymers,^[13–16] in photosensitive glasses,^[17] and in zeolite crystals containing silver clusters.^[18,19] The ideal candidate for perennial 3D optical recording would be a material presenting the high stability and durability of a glass combined with the intense fluorescence of silver clusters. This material has been identified and is now available.^[20] It is a femto-photo-luminescent (FPL) glass, thus labeled because it exhibits remarkable fluorescence properties after femtosecond laser irradiation.

Silver clusters are created by a pulse train from a near infrared (NIR) femtosecond laser focused with a microscope objective inside a FPL glass (Figure 1a). Such a photosensitive glass belongs to the phosphate family and was initially designed for gamma irradiation dosimetry.^[21,22] In the present case, the composition is slightly modified: It is a zinc phosphate glass containing silver ions^[23] presenting an ultraviolet (UV) absorption band below 280 nm. Detailed descriptions of its fabrication and properties can be found in the Experimental section. Following exposure to a high-repetition-rate femtosecond pulse train, the glass presents a broad excitation band (300–450 nm). When excited by NUV radiation, it emits homogeneous white fluorescence, the properties of which (intensity, spectrum, and lifetime) depend on the irradiation dose (fluence, number of pulses, and repetition rate).^[24] This fluorescence is attributed to the presence of Ag_m^{x+} silver clusters with $m < 10$ the number of atoms and x the ionization degree.^[20,25,26] These silver clusters are created inside the focusing voxel (Figure 1a) and are arranged into a pipe shape along the propagation axis, with a length corresponding to the Rayleigh range and a wall thickness of about 80 nm.^[27] For a given fluence range (from 2 J cm⁻² to 6 J cm⁻²), the silver clusters are produced without significant linear refractive index change (<10⁻⁴), while they exhibit appreciable fluorescence and nonlinear optical properties. This glass

[*] Dr. A. Royon, Dr. M. Bellec, G. Papon, Dr. B. Bousquet, Prof. L. Canioni
Centre de Physique Moléculaire Optique et Hertzienne
University of Bordeaux
351 Cours de la Libération, 33405 Talence (France)
E-mail: l.canioni@cpmoh.u-bordeaux1.fr
K. Bourhis, Dr. T. Cardinal
Institut de Chimie de la Matière Condensée de Bordeaux
University of Bordeaux
87 Avenue du Docteur Schweitzer, 33608 Pessac (France)
Dr. Y. Deshayes
Laboratoire de l'Intégration du Matériau au Système
University of Bordeaux
351 Cours de la Libération, 33405 Talence (France)

DOI: 10.1002/adma.201002413

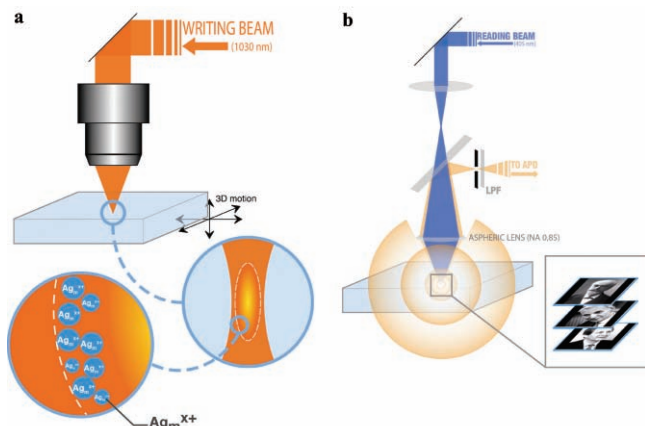


Figure 1. Writing and reading experimental setups. a) A NIR high-repetition-rate femtosecond laser is focused into the glass, which can be moved in 3D by translation stages. By adjusting the dose, silver clusters with perfectly controlled fluorescence features are created at the edge of the focusing voxel. b) A “Blu-Ray” laser diode is focused into the glass. Some of the fluorescence emitted in the entire space by the photo-induced silver clusters is collected by the focusing element, filtered from the excitation with a long pass filter (LPF), and detected with an avalanche photodiode (APD), the setup being in a confocal configuration with the use of a pinhole.

has already shown its potential for 3D optical data storage that takes advantage of the third-order susceptibility contrast of the photo-induced clusters with respect to the glass matrix.^[28]

The fluorescence intensities emitted by the silver clusters can be much higher (50 times) than those from fluorescent molecules such as dyes (Rhodamine 6 G at 10^{-4} mol L⁻¹).^[29] The quantum yield of these species is very high, on the order of 17%.^[30] In the FPL glass, the emission can be tuned from yellow to red.^[20,25] The fluorescence time decay of the clusters is on the order of a few nanoseconds,^[20] allowing a reading speed as high as 500 MHz. In the FPL glass, the fluorescence intensity of the silver clusters varies linearly with the irradiance and logarithmically with the deposited number of pulses, within the range of interest. This last behavior is well known in photographic processes.^[31] Therefore, when the dose is adjusted properly, the fluorescence intensity of the photo-induced species can be controlled exactly as in silver photographic films. Thanks to this material response, grayscale encoding becomes possible. The storage of the information is therefore not based on two levels (binary) but on many levels (e.g., 16 levels, corresponding to hexadecimal). Two approaches can be used to record the words of information: either the fluence or the number of pulses can be adjusted. Here, we choose to present in **Figure 2a** 256 levels of fluorescence intensity by adjusting the number of pulses from 10^2 to 10^7 and keeping the fluence constant at 5 J cm^{-2} . **Figure 2b** shows that the effective reading dynamics is 16 levels, rather than 256. The reading noise is estimated to be 2000 fluorescence counts. Therefore, we choose a sampling of 4000 counts to discriminate two consecutive levels. In order to get a linear fluorescence level scale, the range of number of pulses necessary to record a given level has been adapted with a nonlinear scale. This limited effective reading dynamics is mainly due to the lack of homogeneity of the glass.

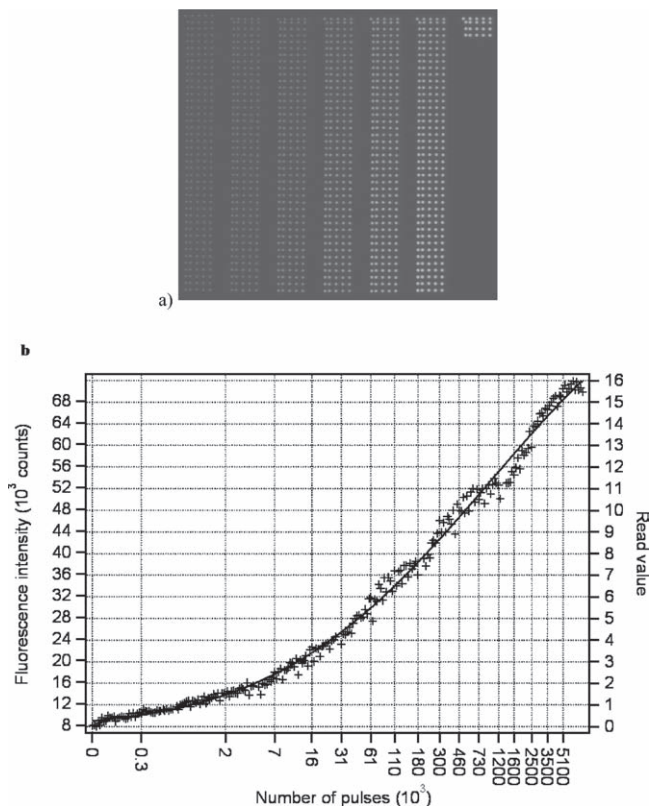


Figure 2. Fluorescence grayscale encoding. a) Confocal fluorescence image ($\lambda_{\text{exc}} = 405 \text{ nm}$) composed of 256 lines of 5 iso-points written with increasing doses. The fluence was kept the same at about 5 J cm^{-2} and the number of pulses was varied from 10^2 (top line of the first column) to 10^7 (bottom line of the seventh column). The fluorescence intensity of each line is measured and depends on the laser dose. b) Evolution of the fluorescence intensity of the 256 lines of **Figure 2a** versus the number of writing pulses. A linear scale of 16 effective gray levels can be extracted, corresponding to a given range of number of writing pulses. The smoothed curve of the experimental data is displayed for visual help. The modulations of the experimental data points from the smoothed curve are due to the inhomogeneity of the reading field of view: Each oscillation relative to the full curve corresponds to a jump from one column to another.

In the present work, the small volume of the synthesized glass guarantees a homogeneity of the composition on the order of 1%. Obviously, this homogeneity could be improved by increasing the batch volume. This is one solution to increase the data storage capacity of this medium.

To illustrate the recording performances according to the principle explained before, a word pattern embedded in the glass was written with a NIR femtosecond laser and read with NUV light. The sample was irradiated with a fixed laser fluence of about 5 J cm^{-2} and the number of pulses varied from 10^2 to 10^7 . The data were embedded 150 μm inside the sample. It contained a pattern of 100×100 pixels with a pixel spacing of 3 μm . The picture recorded shows Claude Cohen-Tannoudji (**Figure 3a**), the 1997 French Nobel laureate in physics for laser cooling of atoms. Using a confocal fluorescence microscope, the image was viewed and is presented in **Figure 3b**. The effective contrast of the recorded image seems to be degraded

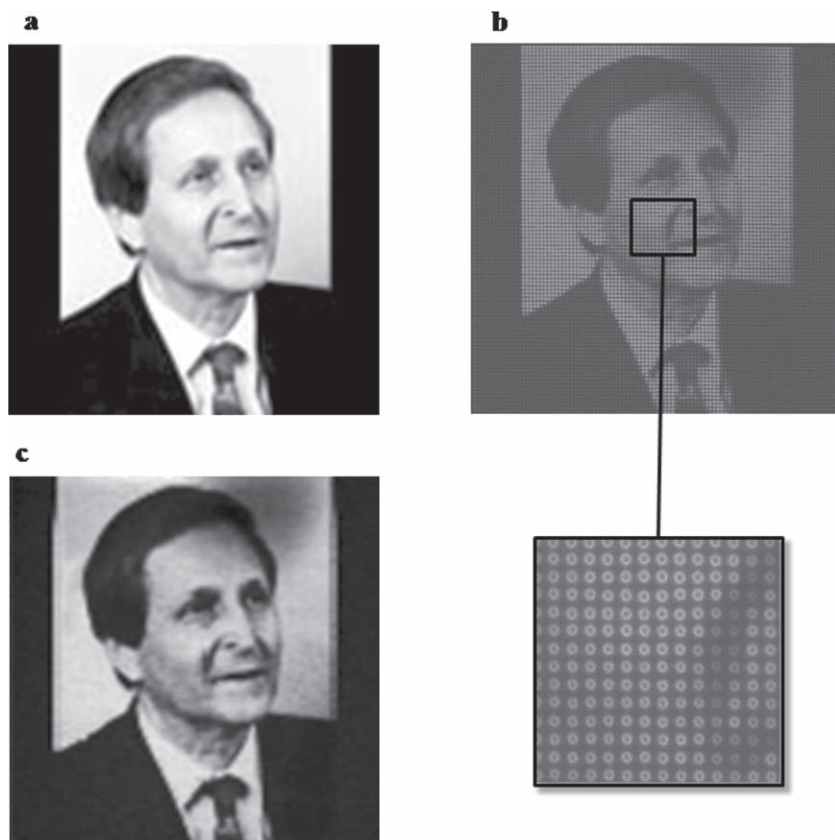


Figure 3. Original, recorded, and decoded images of Claude Cohen-Tannoudji, the 1997 French Nobel laureate in physics. a) The original image is 100×100 pixels and encoded on 256 gray levels. b) The recorded image viewed by confocal fluorescence microscopy ($\lambda_{\text{exc}} = 405$ nm). Inset: The pixels consist of fluorescent rings. The pixel spacing is $3 \mu\text{m}$, the pixel diameter is $2 \mu\text{m}$, and the encoding is 256 gray levels. The image size is $300 \mu\text{m} \times 300 \mu\text{m}$. The fluence was kept constant (5 J cm^{-2}), and the number of pulses varied from 10^2 to 10^7 . c) The decoded image is displayed on the usual 256 levels.

compared to the original image because of the low filling, about $1/3$. Indeed, each word of information is separated by $3 \mu\text{m}$ and corresponds to a fluorescent ring feature, empty in the center (Figure 3b, inset). Note that at lower irradiation dose (number of pulses = 10^7 ; fluence $\leq 3 \text{ J cm}^{-2}$), it is possible to confine the fluorescent structure to the middle of the focal point in order to form a spot rather than a ring.^[20] However, with a writing fluence lower than 3 J cm^{-2} , the range of irradiation dose (number of pulses in this case) to induce fluorescent structures becomes narrower and therefore limits the number of available gray levels. In Figure 3c, each word is reconstructed and coded on 1 hexadecimal. This image is nearly identical to the original when compared. Nevertheless, it exhibits pixelization, as expected with only 16 levels of effective dynamics.

The small variation in the linear refractive index ($< 10^{-4}$), and therefore low scattering, allows the storage to be extended from 2D to 3D. To illustrate this, three layers of data were embedded $150 \mu\text{m}$ inside the sample. Each layer contained a pattern of 100×100 pixels with a pixel spacing of $3 \mu\text{m}$. The pictures of three French Nobel laureates in physics (Gabriel Lippmann in 1908 for a colour photography process, Alfred Kastler in 1966 for optical pumping, and Claude Cohen-Tannoudji) were recorded

in the first, second, and third layers, respectively, with a layer spacing of $20 \mu\text{m}$ in the z -direction. Using a confocal fluorescence microscope, the three layers were imaged and are presented in Figure 4. As expected by the confocal geometry, an image with high contrast and no cross-talk can be viewed. The main advantage of this technique compared to usual 3D data storage is the availability of many layers without any cross-talk. The number of layers is mainly limited by the reading optical setup.

To show the unique behavior of this glass, a silver-containing silicate glass and a commercially available radio-photo-luminescent (RPL) glass containing less than 1 at% silver were also irradiated. The compositions and properties of these glasses can be found in the Experimental section. Similar nanostructures were created as already described for the phosphate glass host, but the stability was reduced to a few minutes under sufficiently intense NUV exposure. This different behavior comes from the stabilization of the released holes within the glass matrix. In the silver zinc phosphate glass, the holes are stabilized because of the long length of the phosphate chains, whereas in the silver silicate glass and the RPL glass, the holes migrate by hopping and finally recombine with the clusters to anneal the fluorescence. As a result, there is no photobleaching of the fluorescence in the FPL glass, which is an indisputable advantage for fluorescence data storage.

In our experimental conditions (encoding dynamics 16 levels, 4 bits; bit spacing $3 \mu\text{m}$; layer spacing $20 \mu\text{m}$), 20 Gbit cm^{-3} could be stored inside the glass. The “Blu-ray” technology uses a reading laser diode at 405 nm and a 0.85 NA (numerical aperture) focusing lens (Figure 1b). The lateral and axial resolutions of a confocal microscope using these devices are $\Delta r = 0.4\lambda_0/\text{NA} = 190 \text{ nm}$ and $\Delta z = 1.4\lambda_0/(\text{NA})^2 = 785 \text{ nm}$, respectively. Considering 8-bit encoding dynamics (256 levels), the maximum storage capacity is about 280 Tbit cm^{-3} . This number could even be increased by the use of laser diodes with shorter wavelengths and higher NA lenses, which will be available in the future and allow an improved space confinement. Besides, a decrease of the laser diode wavelength would permit an increase of the fluorescence efficiency of the clusters (since the maximum of the absorption band is at about 350 nm) and thus enlarge the encoding dynamics.

For use in optical data storage, the recording medium must present a high tolerance to temperature, ageing, and humidity. The stability of the photo-induced silver clusters in FPL glass has therefore been investigated, similarly as in previous work by De Cremer et al. for silver clusters in zeolites.^[32] First, annealing the exposed glass at temperatures from $100 \text{ }^\circ\text{C}$ up to $350 \text{ }^\circ\text{C}$ for 3 h showed no dissociation of the clusters. The temperature

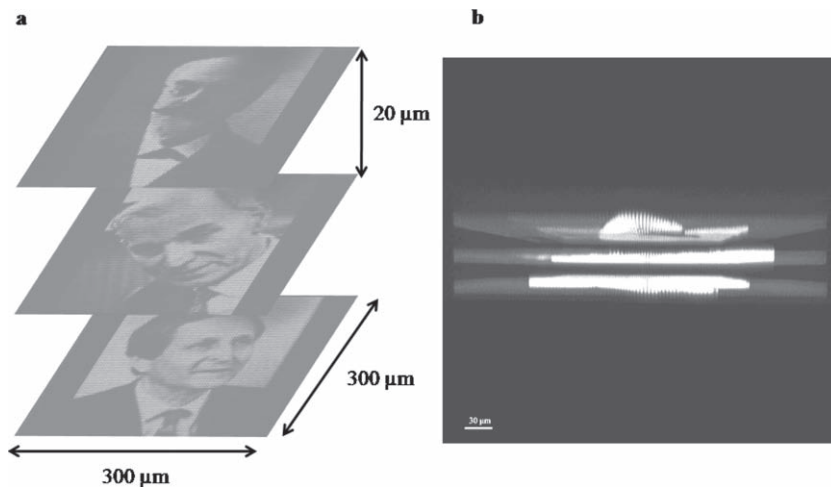


Figure 4. Recorded images viewed by confocal fluorescence microscopy ($\lambda_{\text{exc}} = 405 \text{ nm}$) of three French Nobel laureates in physics: Gabriel Lippmann (1908), Alfred Kastler (1966), and Claude Cohen-Tannoudji (1997). a) The images are 100×100 pixels. The pixel spacing is $3 \text{ }\mu\text{m}$, the pixel diameter is $2 \text{ }\mu\text{m}$, the layer spacing is $20 \text{ }\mu\text{m}$, and the encoding is 256 gray levels. The image size is $300 \text{ }\mu\text{m} \times 300 \text{ }\mu\text{m}$. The fluence was kept constant (5 J cm^{-2}) and the number of pulses was varied from 10^2 to 10^7 . b) Side view of the recorded images. No cross-talk between the layers is observed.

tolerance ($350 \text{ }^\circ\text{C}$) of this recording medium is much higher than the technical standard usually imposed for data storage, that is, $80 \text{ }^\circ\text{C}$. Second, under blue light exposure (ca. 100 kW cm^{-2} at 405 nm and at 370 nm) for hours, corresponding to billions of reading cycles, no change in the fluorescence properties (intensity and spectrum) or in the cluster distribution was observed. Besides, structures written in a FPL glass four years ago and stored without particular precautions are still readable, and their fluorescence is as intense as at that time. Third, the dissolution behavior was studied in similar glass matrices. In particular, in phosphate^[33] and zinc phosphate^[34] matrices, the dissolution rate is on the order of $1 \text{ g cm}^{-2} \text{ min}^{-1}$. These measurements show that the tolerance to humidity of these glass matrices is compatible with data storage applications.

In conclusion, we have demonstrated 3D optical recording in a FPL glass. The fluorescence intensity of the photo-induced clusters is controlled via the exposure conditions of the glass and can be grayscale encoded. This medium presents all the advantages needed for 3D optical data storage: commercial availability of the driver (Blu-ray for example), high storage capacity (up to hundreds of Tbit cm^{-3}), no photobleaching of the fluorescence, no cross-talk, and high reading speed (500 Mbit s^{-1}). Furthermore, the temperature, ageing, and humidity tolerance of this recording medium make it suitable for perennial storage over many centuries.

Experimental Section

Glass Preparation: The glasses were made using a standard melt quench technique. Glass constituents in powder form were used as raw materials and the proper amount was placed in a platinum crucible. A heating rate of about $1 \text{ }^\circ\text{C min}^{-1}$ was used up to $1000 \text{ }^\circ\text{C}$. The melt was then kept at this latter temperature ($1000 \text{ }^\circ\text{C}$) for 24–48 h. Following this step, the liquid was poured into a brass mold after a short increase of

the temperature to $1100 \text{ }^\circ\text{C}$ in order to reach the appropriate viscosity. The glass samples obtained were annealed at $320 \text{ }^\circ\text{C}$ ($55 \text{ }^\circ\text{C}$ below the glass transition temperature) for 3 h, cut ($0.5\text{--}1 \text{ mm}$ thick) and optically polished.

The silver zinc phosphate glass and the silver silicate glass have the following compositions, respectively: $40\text{P}_2\text{O}_5\text{--}4\text{Ag}_2\text{O--}55\text{ZnO--}1\text{Ga}_2\text{O}_3$ (mol%) and $69.98\text{SiO}_2\text{--}1.27\text{Ag}_2\text{O--}16.37\text{Na}_2\text{O--}12.38\text{CaO}$ (mol%). These glasses possess an absorption cutoff wavelength at 280 nm (due to the absorption band associated with the silver ions at around 260 nm) and emit fluorescence mainly around 365 nm when excited at 260 nm . This intrinsic fluorescence is due to Ag^+ ions isolated in the glass.

Sample Exposure: The glass samples were irradiated using a femtosecond laser oscillator source (t-Pulse 500, Amplitude-Systèmes) emitting 500 fs , 10 MHz repetition rate pulses at 1030 nm . The laser mode is TEM_{00} , $M^2 = 1.2$, and the output polarization is TM. The maximum output average power is close to 6 W , which results in a maximum energy per pulse of 600 nJ . Acousto-optic filtering permits the tuning of the pulse energy, the number of pulses, and the repetition rate for control of the cumulated effects. The laser beam was focused using a microscope objective (Zeiss Plan Achromat $40\times$; $\text{NA} = 0.75$) at a depth of $150 \text{ }\mu\text{m}$ in the glass. The beam waist was estimated to be

$0.7 \text{ }\mu\text{m}$. The sample was manipulated using a micro-precision xyz stage (Micro Controle MFA-CC) with a repeatability of $2 \text{ }\mu\text{m}$.

Fluorescence Images and Measurements: The fluorescence imaging was performed with a confocal fluorescence microscope (Leica DMR TCS SP2 AOBS). The excitation was carried out with a laser diode at 405 nm and an oil focusing objective (Leica $40\times$; $\text{NA} = 1.25 \text{ OIL}$; coverslip corrected). The images were 4096×4096 pixels and encoded on 8 bits.

Acknowledgements

The authors acknowledge Philippe Legros, Christel Poujol, Sébastien Marais, Laure Malicieux, and the BIC (Bordeaux Imaging Center) for the confocal fluorescence microscopy. Special thanks are addressed to Isabelle Vabre from IRSN for fruitful discussions. This work has been supported by the Conseil Régional d'Aquitaine and the GIS AMA.

Received: July 5, 2010
Revised: August 30, 2010
Published online: October 19, 2010

- [1] E. Spitz, F. Laloë, J.-C. Hourcade, Life-Expectancy for Digital Data http://www.academie-sciences.fr/publications/rapports/pdf/rapport_infonum_2010_gb.pdf (accessed September 2010).
- [2] M. L. Lee, X. S. Miao, L. P. Shi, *Jpn. J. Appl. Phys.* **2008**, *47*, 6025.
- [3] J. F. Heanue, M. C. Bashaw, L. Hesselink, *Science* **1994**, *265*, 749.
- [4] J. H. Strickler, W. W. Webb, *Opt. Lett.* **1991**, *16*, 1780.
- [5] P. Zijlstra, J. W. M. Chon, M. Gu, *Nature* **2009**, *459*, 410.
- [6] H. Ditzlacher, J. R. Krenn, B. Lamprecht, A. Leitner, F. R. Aussenegg, *Opt. Lett.* **2000**, *25*, 563.
- [7] S. Alasfar, M. Ishikawa, Y. Kawata, C. Egami, O. Sugihara, N. Okamoto, M. Tsuchimori, O. Watanabe, *Appl. Opt.* **1999**, *38*, 6201.
- [8] S. Pan, A. Shih, W. Liou, M. Park, J. Bhawalkar, J. Swiatkiewicz, J. Samarabandu, P. N. Prasad, P. C. Cheng, *Scanning* **1997**, *19*, 156.

- [9] S. Kawata, Y. Kawata, *Chem. Rev.* **2000**, *100*, 1777.
- [10] D. Day, M. Gu, *Appl. Opt.* **1998**, *37*, 6299.
- [11] H. Jiu, H. Tang, J. Zhou, J. Xu, Q. Zhang, H. Xing, W. Huang, A. Xia, *Opt. Lett.* **2005**, *30*, 774.
- [12] J. A. Squier, M. Müller, *Appl. Opt.* **1999**, *38*, 5789.
- [13] H. E. Pudavar, M. P. Joshi, P. N. Prasas, B. A. Reinhardt, *Appl. Phys. Lett.* **1999**, *74*, 1338.
- [14] C. C. Corredor, Z. L. Huang, K. D. Belfield, *Adv. Mater.* **2006**, *18*, 2910.
- [15] K. Braeckmans, S. C. De Smedt, C. Roelant, M. Leblans, R. Pauwels, J. Demeester, *Nat. Mater.* **2003**, *2*, 169.
- [16] F. Fayazpour, B. Lucas, N. Huyghebaert, K. Braeckmans, S. Derveaux, B. G. Stubbe, J.-P. Remon, J. Demeester, C. Vervaet, S. C. De Smedt, *Adv. Mater.* **2007**, *19*, 3854.
- [17] E. Pavel, I. N. Mihaiescu, A. Hening, V. I. Vlad, L. Tugulea, L. Diamandescu, I. Bibicu, M. Chipara, *Opt. Lett.* **1998**, *23*, 1304.
- [18] G. De Cremer, Y. Antoku, M. B. J. Roeflaers, M. Sliwa, J. Van Noyen, S. Smout, J. Hofkens, D. E. De Vos, B. F. Sels, T. Vosch, *Angew. Chem. Int. Ed.* **2008**, *47*, 2813.
- [19] G. De Cremer, B. F. Sels, J.-I. Hotta, M. B. J. Roeflaers, E. Bartholomeeusen, E. Coutino-Gonzales, V. Valtchev, D. E. De Vos, T. Vosch, J. Hofkens, *Adv. Mater.* **2010**, *22*, 957.
- [20] M. Bellec, A. Royon, K. Bourhis, J. Choi, B. Bousquet, M. Treguer, T. Cardinal, J.-J. Videau, M. Richardson, L. Canioni, *J. Phys. Chem. C* **2010**, *114*, 15584.
- [21] H. Schneckenburger, D. F. Regulla, E. Unsöld, *Appl. Phys. A* **1981**, *26*, 23.
- [22] A. V. Dmitryuk, S. E. Paramzina, A. S. Perminov, N. D. Solov'eva, N. T. Timofeev, *J. Non-Cryst. Solids* **1996**, *202*, 173.
- [23] I. Belharouak, C. Parent, B. Tanguy, G. Le Flem, M. Couzi, *J. Non-Cryst. Solids* **1999**, *244*, 238.
- [24] C. Maurel, T. Cardinal, M. Bellec, L. Canioni, B. Bousquet, M. Treguer, J.-J. Videau, J. Choi, M. Richardson, *J. Lumin.* **2009**, *129*, 1514.
- [25] K. Bourhis, A. Royon, M. Bellec, J. Choi, A. Fargues, M. Treguer, J.-J. Videau, D. Talaga, M. Richardson, T. Cardinal, L. Canioni, *J. Non-Cryst. Solids* **2010**, DOI 10.1016/j.jnoncrystol.2010.03.033.
- [26] G. DeCremer, E. Coutiño-Gonzalez, M. B. J. Roeflaers, B. Moens, J. Ollevier, M. Van der Auweraer, R. Schoonheydt, P. A. Jacobs, F. C. De Schryver, J. Hofkens, D. E. De Vos, B. F. Sels, T. Vosch, *J. Am. Chem. Soc.* **2009**, *131*, 3049.
- [27] M. Bellec, A. Royon, B. Bousquet, K. Bourhis, M. Treguer, T. Cardinal, M. Richardson, L. Canioni, *Opt. Express* **2009**, *17*, 10304.
- [28] L. Canioni, M. Bellec, A. Royon, B. Bousquet, T. Cardinal, *Opt. Lett.* **2008**, *33*, 360.
- [29] L. A. Peyser, A. E. Vinson, A. P. Bartko, R. M. Dickson, *Science* **2001**, *291*, 103.
- [30] T. Vosch, Y. Antoku, J.-C. Hsiang, C. I. Richards, J. I. Gonzalez, R. M. Dickson, *Proc. Natl. Acad. Sci. USA* **2007**, *104*, 12616.
- [31] K. Biedermann, *Appl. Opt.* **1971**, *10*, 584.
- [32] G. De Cremer, E. Coutiño-Gonzalez, M. B. J. Roeflaers, D. E. De Vos, J. Hofkens, T. Vosch, B. F. Sels, *ChemPhysChem* **2010**, *11*, 1627.
- [33] A. Mogus-Milankovic, A. Gajovic, A. Santic, D. E. Day, *J. Non-Cryst. Solids* **2001**, *289*, 204.
- [34] H. Takebe, Y. Baba, M. Kuwabara, *J. Non-Cryst. Solids* **2006**, *352*, 3088.